



Water Richness Evaluation of Coal Roof Aquifers Based on the Game Theory Combination Weighting Method and the TOPSIS Model

Longqing Shi¹ · Yu Li¹ · Jin Han² · Xiao Yang¹

Received: 19 June 2024 / Accepted: 7 November 2024 / Published online: 27 November 2024
© The Author(s) under exclusive licence to International Mine Water Association 2024

Abstract

The water richness of the Neogene and Permian strata between the coal seam and the surface was evaluated to address the problem of water inrush from the roof of the coal seam. We selected ten influencing factors to establish a multi-index water richness evaluation system that comprises three indicators for a mine located in Shandong, China. A water-richness predictive method based on Game Theory combinatorial weighting and a Technique for Order Preference by Similarity to an Ideal Solution (TOPSIS) was proposed, and a water richness evaluation model was established accordingly. We used the entropy weight method (EWM) and the improved criteria importance through intercriteria correlation (CRITIC) to obtain the weights of the indicators and combined them using the Game Theory approach. The results show that the overlying strata mainly affects mining safety in the study area's southern region and the delineated water-rich hazard zone is generally consistent with actual measurements. Finally, three measured points were compared with the predicted results, which proved that the method is accurate and useful, providing a new approach for addressing similar issues at other sites.

Keywords Game theory · TOPSIS · Water richness · Entropy weight method · Improved CRITIC method

Introduction

Coal seam roof water inrushes seriously affect the safety of coal mines (Yang et al. 2023). China's coal mines exhibit exceptionally complex stratigraphic and hydrogeological characteristics. The damage to coal seam roofs induced by mining renders them highly susceptible to alterations in water flow paths and spatial–temporal variations in the influx of water (Shi et al. 2020; Wu 2014). Furthermore, China's coal production has gradually escalated, accompanied by a steadily increasing intensity of mining activities (Tian et al. 2010). Consequently, the prevention and mitigation of water-related disasters in coal mine roof strata is of utmost importance.

The primary methods for assessing water richness include physical exploration techniques and multi-factor integrated analysis (Chen et al. 2023). Over the years, scholars have conducted extensive research on the sedimentary characteristics of aquifers, identifying various factors that influence water enrichment. For instance, Wang employed the network parallel electrical method to assess the water-richness of aquifers and highlighted the limitations associated with the DC resistivity method (Wang et al. 2010). Jiang utilized the direct current electric method to gather geoelectric data of aquifers, offering a means to detect water-richness (Jiang 2020). Xie Yuan and his colleagues were the first to systematically apply sedimentology to groundwater exploration in the Ordos Basin, emphasizing that the groundwater enrichment patterns are jointly influenced by sedimentary facies and other hydrogeological conditions (Xie et al. 2005). Building on the water-richness index method, Wu Qiang and his team further incorporated the sedimentary water-control law, considering the comprehensive impact of multiple factors to establish a quantitative evaluation framework for assessing the water richness of loose aquifers beneath the Quaternary system (Wu et al. 2017). Additionally, various scholars have assessed aquifer water-richness using different approaches, including grey theory (Zhang

✉ Jin Han
897958100@qq.com

¹ College of Earth Sciences and Engineering, Shandong University of Science and Technology, Qingdao 266590, China

² College of Computer Science and Engineering, Shandong University of Science and Technology, Qingdao 266590, Shandong, China

et al. 2018), artificial neural networks (Gong et al. 2018), principal component analysis (Wang et al. 2017), S NMR information fusion (Huang et al. 2018), and AVO technology (Tian et al. 2017), among others.

The core principle of the comprehensive evaluation method for predicting aquifer water richness lies in establishing an index system that encompasses the factors that influence water richness and determining the extent of each index's influence through techniques such as the analytic hierarchy process (AHP) and Gray theory. However, existing comprehensive evaluation methods exhibit shortcomings, including insufficient data integration, indicator interaction, and the uncertainty inherent in subjective judgments (Huang 2016; Jiang et al. 2012). Furthermore, most water richness evaluation methods developed for mine water hazards rely heavily on hydrogeological data, and the selection of impact indicators tends to be relatively homogenous, posing challenges for evaluating water richness in coal mine aquifers. Therefore, our objective for this study was to establish a multi-indicator water richness evaluation system based on the analysis of relevant geological data and actual hydrogeological conditions. We then developed a water richness evaluation model based on Game Theory combination weighting and the Technique for Order Preference by Similarity to an Ideal Solution (TOPSIS) model and conducted zonal prediction and water richness evaluation for a mine in Shandong.

Overview of the Study Area

The study area is an alluvial plain in Shandong Province, China: the terrain is high in the southwest and low in the northeast, with gently sloping land, shallow flat depressions, and trough depressions. The hydrological system in the study area is relatively well-developed. The coal-bearing strata belong to the Carboniferous to Permian system. The stratigraphy is controlled by regional faults, which have formed fracture structures, as shown in Fig. 1. The cutting effect of the faults has shortened the distance between the main water-bearing strata and the coal seams, actually bringing them in contact in many places, which increases the likelihood of water inrushes.

The overlying aquifers of the area's coal beds mainly consist of Quaternary gravel aquifers, Neoproterozoic aquifers, and Permian Shihezi Group aquifers from top to bottom, as shown in Fig. 2. The overlying strata have gone through many phases of tectonic movement, and aquifers and aquicludes are stacked on top of each other. Therefore, the risk of water inrush during coal mining must be analyzed.

Analysis of Water Richness Indexes

Through a comprehensive analysis of the geology, hydrogeology, and drill hole data in the study area, the water

barrier capacity index and water inrush intensity index have been established from the aspect of sedimentary water control, and water-conducting channel indexes have been established based on the connectivity of aquifers. These indexes collectively form a water-richness evaluation system. The water influx intensity indexes include the hydraulic pressure of the primary aquifer (B), the lithological coefficient of sandstones (P), the equivalent thickness of sandstones (M), and the interval between the Neogene System and the coal seam (J). The water barrier capacity indexes consist of the thickness of the clay layers (T) and the number of sandy-clay interlayers (N). The water-conducting channels indexes consist of the height of water-conducting fracture zones (H), the fault strength index (Y), the fault fractal dimension value (D), and the fault density (C), as shown in Fig. 3.

Water Barrier Capacity Index

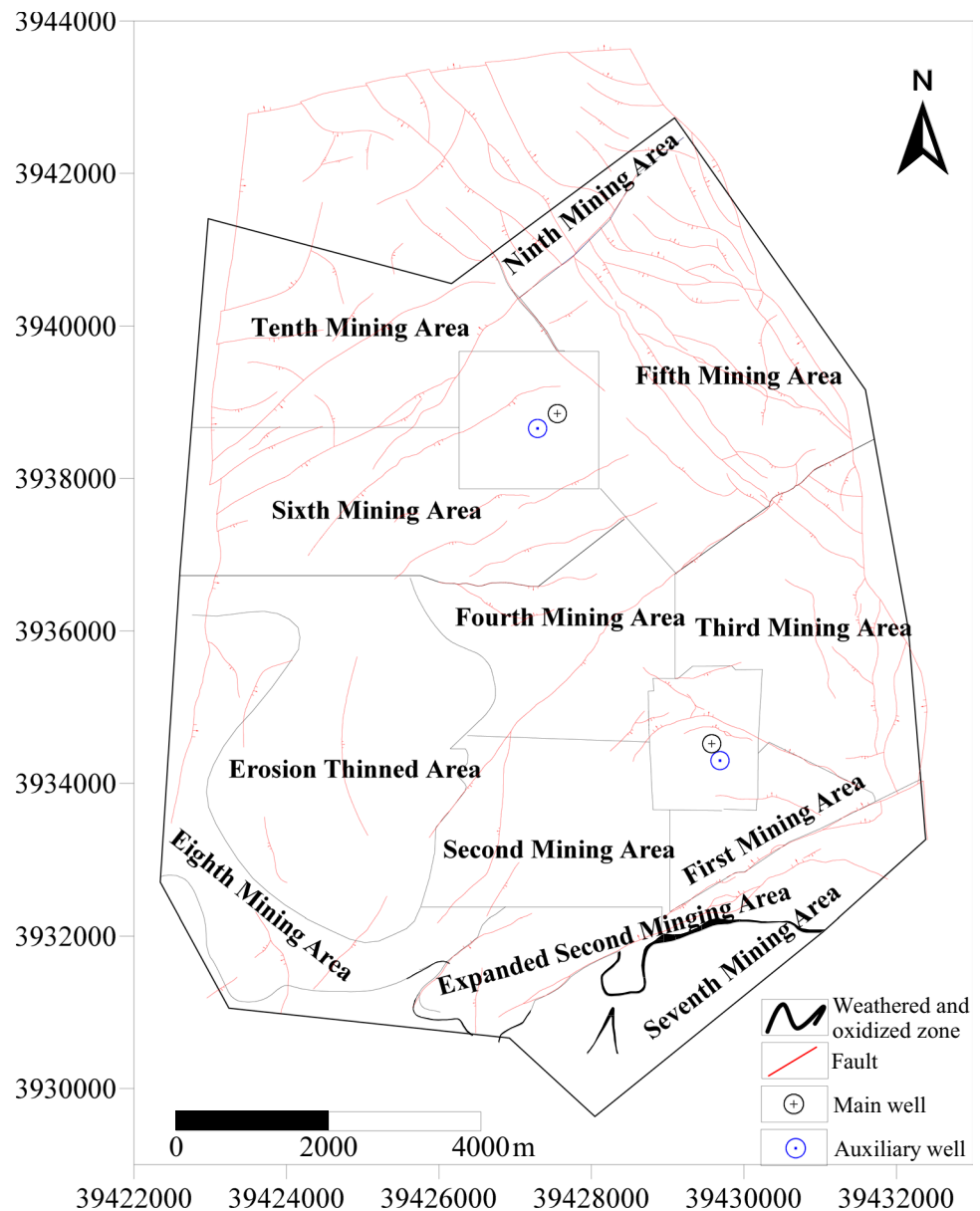
The number of sand-clay interlayers (N) refers to the number of water-bearing gravel, coarse sand, medium sand, fine sand, and silt layers alternating with clay layers in the Cenozoic strata. Based on the geological report, the sediments in the study area are primarily clay-based. It is believed that the greater the number of sand-clay interlayers, the better the water-barrier properties and the poorer the water-rich conditions. Based on Fig. 4a, it can be seen that there are more sand-clay interlayers is larger in the western, southwestern, and southern parts of the wellfield.

The thickness of the Cenozoic clay layer is a very direct response to the water-richness of the stratigraphy in the section. A greater thickness of clay layers (T) results in a thinner relative aquifer and a less water-rich formation. From Fig. 4, it can be seen that the clay layer is thicker in the central, southwestern, and eastern parts of the study area; the clay layer is thinner in the northern part.

Water Inrush Intensity Index

The hydraulic pressure of the primary aquifer (B) is a critical factor in the assessment of groundwater systems. It refers to the pressure exerted by the water within the aquifer, which is influenced by the aquifer's depth, the volume of water it contains, and the surrounding geological formations. High hydraulic pressure can indicate a large amount of stored water and can affect the movement and availability of groundwater. Typically, the greater the hydraulic pressure of the primary aquifer, the greater its water richness. As shown in Fig. 5a, the hydraulic pressure of the primary aquifer in the southern part of the study area is relatively high.

Fig. 1 Schematic diagram of the research area overview



The lithological coefficient of sandstones (P) is the proportion of the Cenozoic stratigraphy accounted for by the loosely bedded water-bearing gravel, coarse sand, medium sand, fine sand, and silt layers. In general, the greater the percentage of thickness of these five types of sandstone aquifers, the more water-rich the site. According to Fig. 5b, it can be seen that the sandstone lithology coefficients are larger in the southern and central part of the study area.

The interval between the Neogene System and coal seam (J) is the vertical height difference between the bottom interface of the Neogene System and the top plate of the coal seam. Analysis of stratigraphic data from the mining field in that a coal seam outcropped in the southern part of the mining field. Due to weathering and erosion, the rock layers in this area have become soft, forming an oxidized zone in

this area. Therefore, the interval between the Neogene System and the coal seam is a critical indicator for evaluating water richness and directly reflects the impact of the overall distribution of Permian strata on coal seam mining.

Contour mapping of the interval between the Neogene System and coal seam based on drill hole data is shown in Fig. 5c. The smaller the interval between the Neogene System and coal seam, the higher the water richness hazard index. As can be seen from the figure, the base of the Neoproterozoic strata and the roof of the coal seam contact in the blue area in the southern part of the well field, which is the erosion zone of the coal seam outcrop.

Sandstone is one of the important factors in evaluating water enrichment, as its thickness directly correlates with water richness; the thicker it is, the richer it is in water.

Fig. 2 Stratigraphic schematic of the study area

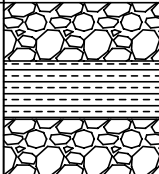
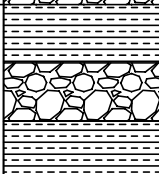
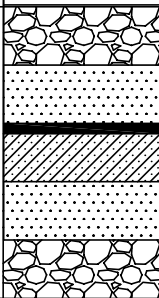
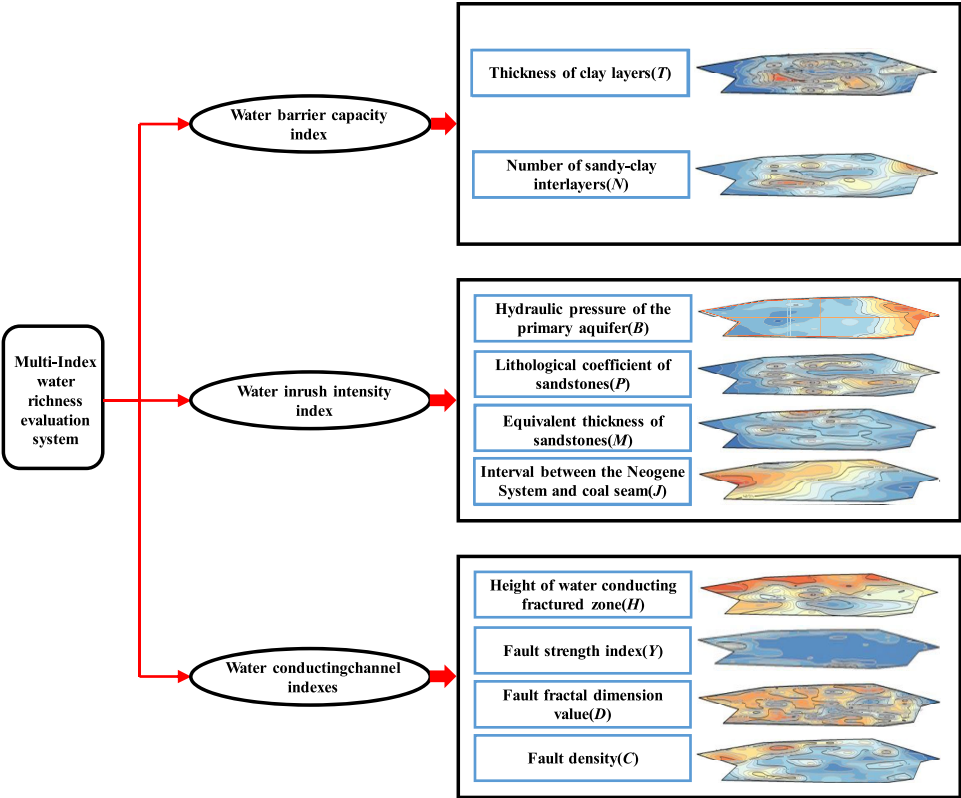
Stratigraphic unit		Bar chart	Average thickness	Coal formation and Principal aquifer	Lithology
Era	Series				
Kz	Q		119.14m	Quaternary sandy gravel porous aquifer	Primarily sand and gravel with clay
	N		287.06m	Neogene aquifer	Primarily sand and gravel with clay
Pz	P		276.24m	Permian Shihezi Group aquifer and coal seam	Dominated by sandstone, mudstone, and siltstone

Fig. 3 Multi-Index water richness evaluation system



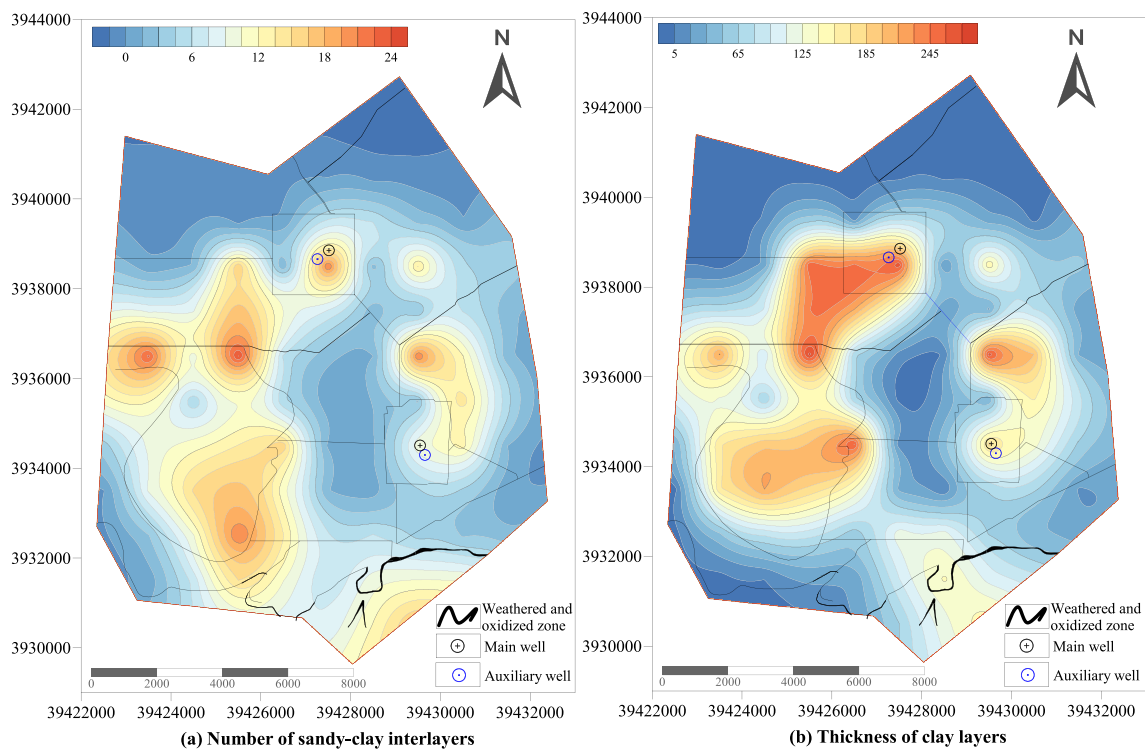


Fig. 4 Contour map of the Water barrier capacity index

However, in water richness evaluation studies, the disparities in porosity and permeability among coarse, medium, and fine sandstones are frequently overlooked, resulting in outcomes that deviate from reality (Wei et al. 2020). In this study, the concept of sandstone equivalent thickness (M) was incorporated into the water-richness evaluation model, employing the porosity ratio of sandstone as a conversion factor to transform thicknesses of coarse-, medium-, and fine-grained sandstones into a unified sandstone equivalent thickness. The formula is as follows:

$$M = M_c + k_1 M_m + k_2 M_f \quad (1)$$

where M is the equivalent thickness of sandstone; M_c , M_m , M_f are the true thicknesses of coarse-, medium-, and fine-grained sandstone respectively; k_1 is the thickness conversion equivalence factor for medium-grained sandstone; and k_2 is the conversion equivalence factor for the thickness of fine-grained sandstone. Using the porosity of coarse-grained sandstone as a reference point (designated as 1), the equivalent conversion coefficients for medium- and fine-grained sandstone can be determined based on the porosity measurements of the Permian formations, resulting in $k_1 = 0.8$ and $k_2 = 0.6$. The greater the equivalent thickness of the sandstone, the greater the risk of water enrichment in the area. As illustrated in Fig. 5d, it is evident that the equivalent

thickness of sandstone is greater in both the eastern and northern sections of the study area.

Water Conducting Channel Indexes

In this paper, the entire area of the fracture structure is divided into the same 143 small grids for counting the parameters required for each indicator.

The Height of the Water-Conducting Fractured Zone

The water-conducting fractured zone is a channel created by mining activities and serves as the primary water-conducting pathway that leads to water influx in mines. The height of the water-conducting fractured zone (H) will directly affect the risk of water inrush in coal mines. We assume that the strata overlying the coal seam are of moderate hardness, allowing the formula for the height of the water-conducting fracture zone in the coal seam to be expressed as:

$$H = \frac{100 \sum M}{1.6 \sum M + 3.6} + 5.6 \quad (2)$$

where H is the height of the water-conducting development zone, in m, and $\sum M$ is the cumulative mining thickness, in m. The taller the hydraulic fracture zone, the greater the

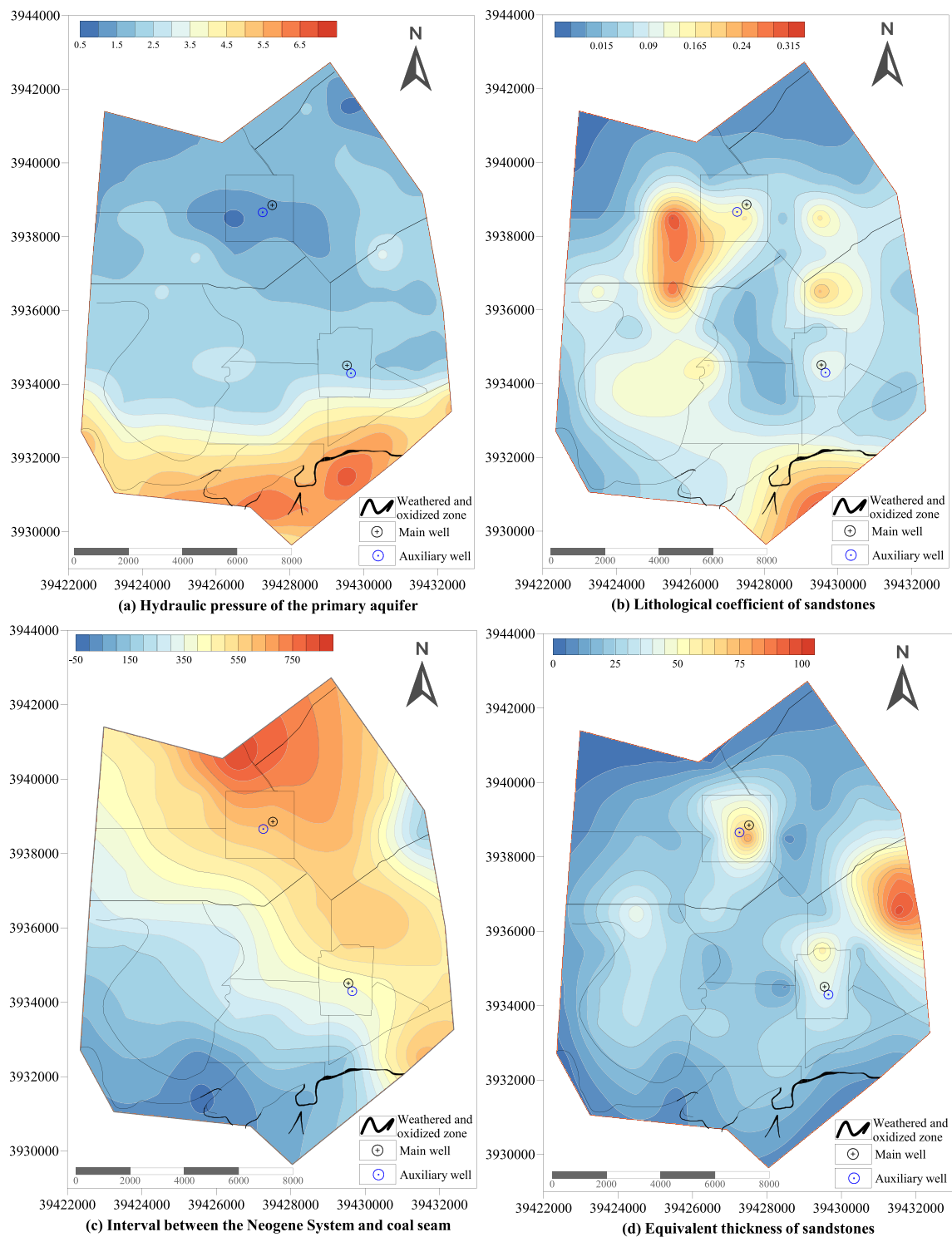


Fig. 5 Contour map of the water inrush intensity index

likelihood of a water inrush. As depicted in Fig. 6a, it is evident that the height of the water-conducting fissure zone is more prominent in the eastern, northeastern, and north-western sections of the study area.

Fault Strength Index

The fault strength index (Y) represents the sum of the products of the lengths and drops of all faults within a unit

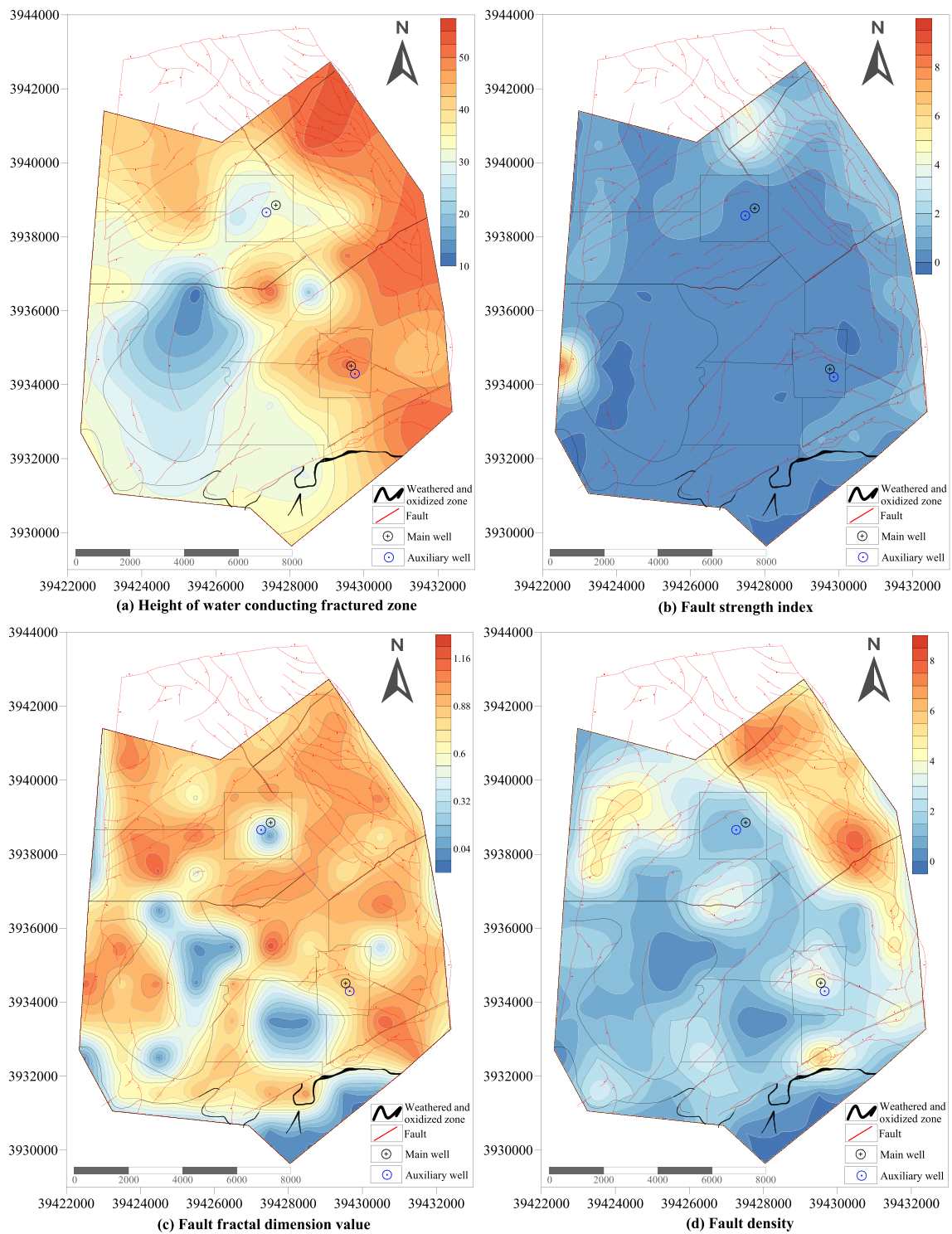


Fig. 6 Contour map of the water conducting channel indexes

area, effectively reflecting the degree of fault development. A higher value of this index indicates a greater impact and complexity of faults within the unit area. The formula for its calculation is as follows:

$$Y = \frac{\sum_{i=1}^n H_i \times L_i}{S} \quad (3)$$

where Y represents the fault strength index; n represents the total number of faults within the statistical unit; L_i denotes

the extension of the i th fault within the grid, in km; H_i denotes the drop of the i th fault within the grid, in km; and S represents the area of the divided grid unit, in km². Analysis of Fig. 6b indicates that only a small portion the western part of the study area has a higher fault intensity index.

Fault Fractal Dimension Value

Fault fractal dimension value (D) encompasses various aspects of change relationships such as the number of faults, their extension lengths, and their intersecting relationships. It can serve as a comprehensive indicator that fully reflects the degree of development of fault structures (Shi et al. 2022). A higher fault fractal dimension value indicates greater complexity of faults within a unit area, leading to greater aquifer connectivity. In this paper, the complexity of the structural grid was studied through similarity dimension. The formula is as follows:

$$D = -\frac{\lg N(r)}{\lg r} \quad (4)$$

where $N(r)$ is the number of faults intersecting grids of different lengths and r is the side length of each grid, in m. As can be seen from Fig. 6c, except for a small area in the central part of the study area, the fault fractal dimension values in other regions are relatively large, which is consistent with the distribution of fault structures indicated by the red line.

Fault Density

The fault density (C) refers to the number of faults per unit area. The formula is as follows:

$$C = \frac{N}{S} \quad (5)$$

where C is fault density, in number of faults per km²; N is the total number of faults; and S is the area, in km². A higher fault density indicates a greater number of faults within a region, resulting in more abundant water-conducting channels. Based on the analysis of Fig. 6d, the northeastern part of the study area has a relatively high fault density, indicating a denser development of faults.

Methodology

In selecting the approach for evaluating the water richness of the overlying strata of the coal seam and determining the mathematical model, various coal mine risk factors had to be accounted for, as different hazards can lead to various degrees of disaster severity. Next, since evaluation of the water richness of the strata overlying the coal seam is

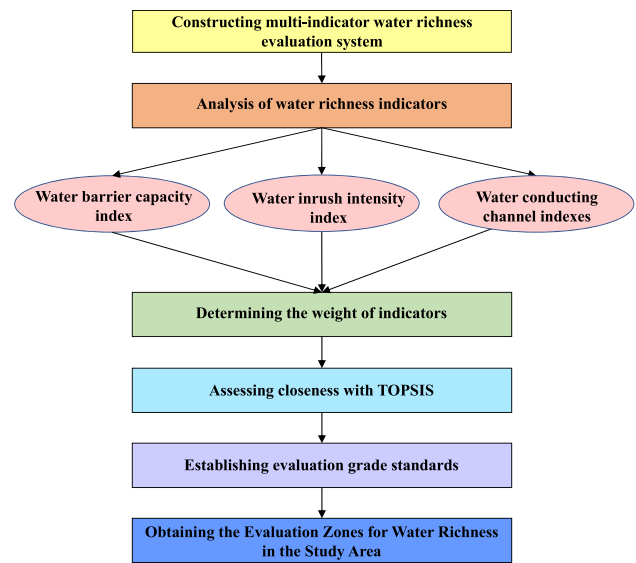


Fig. 7 Flowchart of water richness evaluation

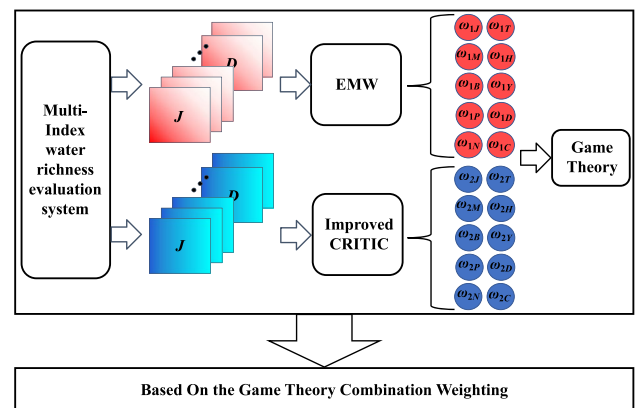


Fig. 8 Indicator weighting process

complex and overlapping, a comprehensive weighting of each evaluation index from multiple perspectives was necessary. Finally, based on a comprehensive determination of the weighting of indicators and evaluation methods, we established a water richness evaluation model by combining the game theoretic combinatorial weighting and the TOPSIS methods, as shown in Figs. 7 and 8.

Entropy Weight Method

In this method, which Shannon (1948) proposed, the final design selection is free from any external interference, and the selection process is solely limited to the data presented in the decision matrix (Yazdani et al. 2023). The entropy weight method (EWM) is an objective weighting

approach that determines the weight coefficients based on the degree of variation in the information utility values of each evaluation indicator. The smaller the entropy of the indicator information, the greater the degree of variation, which means it is more important in the evaluation, resulting in a larger weight. Conversely, the larger the entropy of the information, the smaller the weight (Zuo et al. 2020). The entropy weight method has great advantages in evaluation indicator systems with a large number of indicators and a long time span (Zhang and He 2024). The main steps are as follows:

- (1) Construct the original evaluation indicator matrix X
Assuming there are m evaluation indicators and n evaluation objects, where x_{ij} represents the corresponding value of the i th evaluation indicator for the j th evaluation object, the original evaluation matrix is constructed as follows:

$$X = (x_{ij})_{m \times n} \quad (i = 1, 2, \dots, m; j = 1, 2, \dots, n) \quad (6)$$

- (2) Normalization and positive transformation
Due to the differences in types and dimensions of various indicators, it is necessary to perform dimensionless processing on each indicator to eliminate the impact of these differences. For EWM, it is advisable to adopt the extreme value method for processing to obtain a standardized matrix Y (Zhu and Wei 2015):

$$Y = (y_{ij})_{m \times n} \quad (i = 1, 2, \dots, m; j = 1, 2, \dots, n) \quad (7)$$

where Y is the standardized matrix; y_{ij} is the standardized value of the j th evaluation object on the i th evaluation indicator. Thus:

$$\text{Maximization - oriented indicator : } y_{ij} = \frac{\max(x_{ij}) - x_{ij}}{\max(x_{ij}) - \min(x_{ij})} \quad (8)$$

$$\text{Minimization - oriented indicator : } y_{ij} = \frac{\max(x_{ij}) - x_{ij}}{\max(x_{ij}) - \min(x_{ij})} \quad (9)$$

where y_{ij} is the standardized value of the j th evaluation object on the i th evaluation indicator.

- (3) Calculate the information entropy of the i th evaluation indicator

$$h_i = \frac{1}{\ln n} \sum_{j=1}^n \ln e_{ij} \quad (10)$$

$$e_{ij} = \frac{y_{ij}}{\sum_{j=1}^n y_{ij}} \quad (11)$$

where h_i is the entropy of the i th indicator and e_{ij} is the standardized value of the i th indicator for the j th evaluation object.

- (4) Calculate the weights

$$\omega_{li} = \frac{1 - h_i}{m - \sum_{i=1}^m h_i} \quad (12)$$

where ω_{li} is weight of the i th indicator.

Improved CRITIC Method

The CRITIC method (criteria importance through intercriteria correlation), proposed by Diakoulaki et al. (1995), is an objective weighting method that comprehensively measures the weight of indicators by calculating their variability and conflict. The variability refers to the difference in values taken by the same indicator for different objects, which is measured by the standard deviation. The conflict mainly refers to the correlation among evaluation indicators, which is measured by the correlation coefficient. The universally applied calculation method of the CRITIC method has two issues (Zhang and Zhang 2015; Zhang et al. 2020):

- (1) Due to differences in the dimensions and magnitudes of various indicators, using the standard deviation to reflect variability may result in low accuracy and significant errors.
- (2) The correlation coefficient between indicators can potentially assume negative values. Nevertheless, positive and negative correlations with identical absolute values should exhibit equivalent degrees of correlation, albeit in opposing directions.

Therefore, we improved the general calculation method (Wang and Hu 2022) in two ways: we used the coefficient of variation to measure the differences among indicators and calculated the absolute value of the correlation coefficient to evaluate potential conflicts among indicators. Thus, if C_i represents the information quantity of the i th evaluation indicator, its expression formula is:

$$C_i = \frac{\sigma_i}{X_i} \sum_{j=1}^n (1 - |r_{ij}|) \quad (i = 1, 2, \dots, m; j = 1, 2, \dots, n) \quad (13)$$

where σ_i is the standard deviation of the i th evaluation indicator, X_i is the mean value of the i th evaluation indicator, σ_i/X_i is the coefficient of variation for the i th evaluation indicator, and r_{ij} is the correlation coefficient between the i th and the j th evaluation indicators. The calculation formula for the weight ω_{2i} of the i th evaluation indicator is:

$$\omega_{2i} = \frac{C_i}{\sum_{i=1}^m C_i} \quad (i = 1, 2, \dots, m) \quad (14)$$

Game Theory Based Combined Weighting Method.

Game Theory offers a mathematical framework for exploring decision-making processes and optimizing benefits in scenarios where multiple individuals within a group engage in conflict or competition (Yang et al. 2023). Based on Game Theory, the weights obtained from the two preceding methods were integrated to derive a combined weight, calculated as follows (Zhao et al. 2023):

- (1) First, we calculated the weights of each indicator using the entropy weight method and the improved CRITIC method, obtaining weight sets ω_1 and ω_2 , respectively. We then set a_1 and a_2 as the linear combination coefficients and performed a linear combination of the weight sets ω_1 and ω_2 .

$$\omega = a_1 \omega_1^T + a_2 \omega_2^T \quad (15)$$

- (2) Based on the idea of Game Theory, we optimized the linear combination coefficients a_1 and a_2 in the above formula and determined the objective function with the goal of minimizing the deviation between the combined weight ω and ω_1, ω_2 .

$$\min \left\| \sum_{k=1}^2 a_k \omega_k^T - \omega^T \right\|^2 \quad (k = 1, 2) \quad (16)$$

- (3) Based on the properties of a matrix differential, we determined the linear differential equation system for the first-order derivative condition of the above optimization formula.

$$\begin{bmatrix} \omega_1 \omega_1^T & \omega_1 \omega_2^T \\ \omega_2 \omega_1^T & \omega_2 \omega_2^T \end{bmatrix} \begin{bmatrix} a_1 \\ a_2 \end{bmatrix} = \begin{bmatrix} \omega_1 \omega_1^T \\ \omega_2 \omega_2^T \end{bmatrix} \quad (17)$$

- (4) By solving the above formula, we obtained the optimized combination coefficients a_1 and a_2 . Normalization gave us: $a_1^* = a_1/(a_1 + a_2)$ and $a_2^* = a_2/(a_1 + a_2)$. Then, the comprehensive weight ω based on the combination of weights using Game Theory could be calculated:

$$\omega = a_1^* \omega_1^T + a_2^* \omega_2^T \quad (18)$$

the negative ideal solution (Arcanjo et al. 2020). The specific calculation steps are as follows:

- (1) Homogenization and normalization of the original data in the research area: The extremely small water-richness index is processed by reciprocal transformation and then the normalized value is calculated using a formula. This process transforms the original matrix X into a dimensionless decision-making matrix $Z = (z_{ij})_{m \times n}$.

$$z_{ij} = \frac{x_{ij}}{\sqrt{\sum_{i=1}^m x_{ij}^2}} \quad (19)$$

- (2) To construct the weighted decision matrix V , you multiply the standardized matrix Z_{ij} with the weight vector ω obtained through the combination of weights based on Game Theory to derive the weighted decision matrix V .

$$v_{ij} = \omega_i z_{ij} \quad (20)$$

- (3) Calculate the positive and negative ideal solutions, A_i^+ and A_i^- .

$$\begin{cases} A_i^+ = \max_{1 \leq j \leq n} (v_{ij}) & (i = 1, 2, \dots, m) \\ A_i^- = \min_{1 \leq j \leq n} (v_{ij}) & (i = 1, 2, \dots, m) \end{cases} \quad (21)$$

- (4) Calculate the distances between each evaluation object and the positive and negative ideal solutions, Ad_j^+ and Ad_j^- . Then calculate the distances between the evaluated objects and the positive ideal solution A_i^+ and the negative ideal solution A_i^- using the Euclidean distance, respectively.

$$\begin{cases} Ad_i^+ = \sqrt{\sum_{j=1}^m (A_i^+ - v_{ij})^2} & (j = 1, 2, \dots, n) \\ Ad_i^- = \sqrt{\sum_{j=1}^m (A_i^- - v_{ij})^2} & (j = 1, 2, \dots, n) \end{cases} \quad (22)$$

- (5) Then calculate the closeness degree, G_j .

$$G_j = \frac{Ad_j^-}{Ad_j^+ + Ad_j^-} \quad (j = 1, 2, \dots, n) \quad (23)$$

TOPSIS Method

The TOPSIS is a method of multi-criteria decision-making analysis that aims to select the optimal alternative based on its proximity to the ideal solution and remoteness from

In the formula, the closeness degree G_j ranges from 0 to 1, reflecting the closeness of the evaluated water richness indicators to the ideal solution. A higher closeness degree indicates that the evaluation indicators tend to approach the positive ideal solution, indicating greater

water richness. Conversely, a lower closeness degree suggests that the evaluation indicators tend to approach the negative ideal solution, indicating less water richness.

Result and Discussion

Standardization of Data Coordinate Points

The principle of water richness evaluation involves calculating the fusion value of various influencing factors at the same target location within the study area, and subsequently obtaining a fused contour map for the entire mining field. Therefore, based on the zoning classified according to the

statistical data of water conducting channel indexes, the mining field in the study area is divided into 143 identical grids. Using Surfer software, the Z-axis coordinate values of the center points for the 143 grids from each contour map were extracted, as shown in Table 1.

Weights of Water Richness Indexes

(1) EWM weights

By processing the data in Table 1 through Eqs. (6) to (9), we obtained their standardized form. Subsequently, by using Eqs. (10) and (11), the weights were calculated by EWM ω_1 for the derived indicators, as shown in Fig. 9 and Table 2.

Table 1 Simplified data table of evaluation indicators for the study area

No	<i>J</i>	<i>M</i>	<i>B</i>	<i>P</i>	<i>N</i>	<i>T</i>	<i>H</i>	<i>Y</i>	<i>D</i>	<i>C</i>
1	567.40	−5.45	0.8	−0.06	−2.99	−57.29	44.99	0.00	0.00	0.00
2	616.44	−4.89	0.7	−0.06	−3.06	−54.30	46.13	5.20	0.96	1.00
3	662.67	−4.03	1.1	−0.05	−3.11	−51.70	47.35	8.33	0.77	4.00
4	691.32	−2.46	1.3	−0.05	−3.17	−49.68	48.75	8.15	0.88	3.00
5	692.19	−0.19	1	−0.05	−3.24	−48.12	50.36	5.28	0.73	2.00
6	666.91	2.32	1.1	−0.04	−3.28	−46.42	51.85	7.37	0.89	3.00
7	623.03	4.80	2.1	−0.04	−3.22	−43.66	52.76	0.00	0.00	add.00
8	548.79	−3.86	0.6	−0.05	−2.41	−49.04	43.80	6.11	0.86	2.00
9	567.40	−5.45	1.1	−0.06	−2.99	−57.29	44.95	5.32	0.00	4.00
...
135	28.55	3.65	4.6	0.02	2.09	−31.21	32.43	0.00	0.00	0.00
136	20.86	7.60	5.7	0.04	5.71	−22.76	31.35	0.00	0.00	0.00
137	9.02	8.58	6.1	0.06	8.98	−10.33	31.89	0.00	0.00	0.00
138	29.45	11.89	6	0.08	8.03	4.51	33.79	0.20	0.36	2.00
139	67.62	14.40	6.5	0.13	7.88	20.16	34.15	0.00	0.00	0.00
140	105.66	11.27	6	0.22	12.11	64.91	34.37	0.00	0.00	0.00
141	176.69	4.50	5.5	0.33	17.28	118.86	37.86	0.00	0.00	0.00
142	70.80	8.11	3.5	0.17	10.25	151.02	35.46	0.00	0.00	0.00
143	115.34	6.02	4.6	0.25	13.51	65.53	36.59	0.00	0.00	0.00

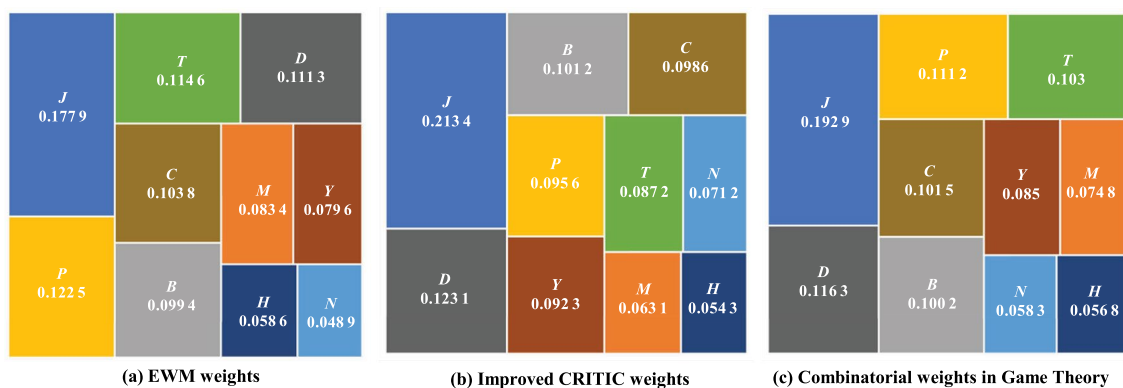


Fig. 9 Weighted tree diagram

Table 2 Weight of water richness indicator

Indicator	ω_1	ω_2	ω	Type of indicator
<i>J</i>	0.1779	0.2134	0.1929	Mini-type
<i>M</i>	0.0834	0.0631	0.0748	Max-type
<i>B</i>	0.0994	0.1012	0.1002	Max-type
<i>P</i>	0.1225	0.0956	0.1112	Max-type
<i>N</i>	0.0489	0.0712	0.0583	Mini-type
<i>T</i>	0.1146	0.0872	0.103	Mini-type
<i>H</i>	0.0586	0.0543	0.0568	Max-type
<i>Y</i>	0.0796	0.0923	0.085	Max-type
<i>D</i>	0.1113	0.1231	0.1163	Max-type
<i>C</i>	0.1038	0.0986	0.1016	Max-type

(2) Improved CRITIC weights

By introducing the original data into Eq. (13), we obtained the information content C_i contained in each evaluation indicator. The larger the value of C_i , the more important the evaluation indicator is considered to be, resulting in a greater weight. Subsequently, by substituting C_i into Eq. (14), we calculated the improved CRITIC method weights ω_2 for the indicators, as shown in Fig. 9 and Table 2.

(3) Based on the Game Theory combination weighting

By incorporating the weights ω_1 derived from EWM method and the weights ω_2 obtained from the improved CRITIC method into Eq. (15), Game Theory was used to determine the final optimized combination coefficients, with $a_1 = 0.5783$ and $a_2 = 0.4217$. By substituting these combination coefficients into Eq. (18), the combined weights ω for each indicator were obtained, as shown in Fig. 9 and Table 2.

Water Richness Evaluation Results

By introducing the original data into Eq. (19), a dimensionless decision matrix Z was obtained. Using the combined weights of each indicator derived earlier, the matrix Z was weighted to produce a weighted decision matrix V . Subsequently, the positive ideal solution A_i^+ and negative ideal solution A_i^- for the water richness of the study area were obtained using Eq. (21). Finally, the distances between each evaluation object and the positive ideal solution Ad_j^+ and the negative ideal solution Ad_j^- were calculated using Eq. (22). From this, the closeness degree G_j can be derived using Eq. (23). In this paper, the closeness degree G_j is used to represent the water-richness of the evaluated objects. A higher G_j value indicates greater water-richness. To present the results more visually, the closeness degree G_j is multiplied by 100 to obtain a water richness score for each evaluated object, as shown in Table 3.

Table 3 Score of water richness evaluation

No	Ad_j^+	Ad_j^-	Score
1	0.192	0.0614	23.9692
2	0.1933	0.0727	27.3833
3	0.1879	0.0695	27.8944
4	0.1852	0.0693	27.2435
5	0.1798	0.063	25.0893
6	0.1823	0.0719	27.4224
7	0.1777	0.0563	26.3064
8	0.1948	0.0685	24.5685
9	0.199	0.0607	27.3352
10	0.1771	0.694	26.8953
...
136	0.1592	0.091	32.8372
137	0.1465	0.0915	42.8104
138	0.1362	0.0926	55.4773
139	0.1371	0.1101	37.9034
140	0.1065	0.1217	42.5538
141	0.1093	0.1532	44.6857
142	0.1131	0.1009	56.329
143	0.1264	0.1332	51.4716

Currently, there is no universal classification standard for water richness evaluation, and it only has relative significance. Therefore, based on the above water richness evaluation results, we employed the equal interval method to assign threshold values to the classification intervals. This approach takes into account the influence and contribution of each indicator on water richness. We then divided the range between the highest and lowest scores from the evaluation into equal intervals, thus obtaining the various score ranges. The water richness indicators are divided into five grades: weak, relatively weak, moderate, relatively strong, and strong, based on their scores from low to high, as shown in Table 4. The higher the score of the evaluated object, the higher the grade, and the stronger the water richness. By combining Tables 3 and 4, we obtained the frequency distribution histogram of water-richness scores as well as the water richness zoning map in the study area, as shown in Figs. 10 and 11.

As can be seen from the map, areas with strong and relatively strong water richness are mainly located in the south and southwest of the mining area, posing a greater risk. There are large areas of moderate water richness zones in the

Table 4 Classification of water richness evaluation grades

Evaluation level	Weak	Relatively weak	Medium	Relatively strong	Strong
Score range	[23, 32.2)	[32.2, 41.4)	[41.4, 50.6)	[50.6, 59.8)	[59.8, 69)

Fig. 10 Frequency distribution histogram of water richness scores in the study area

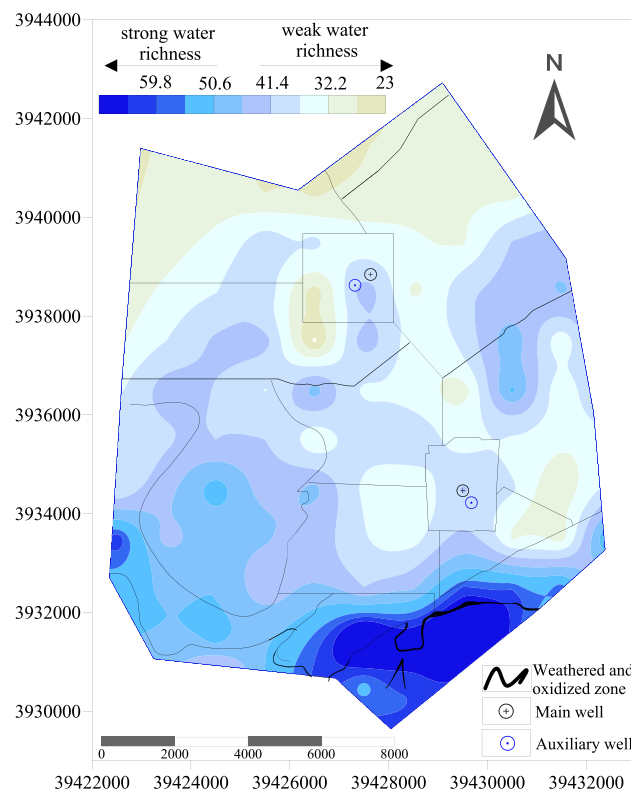
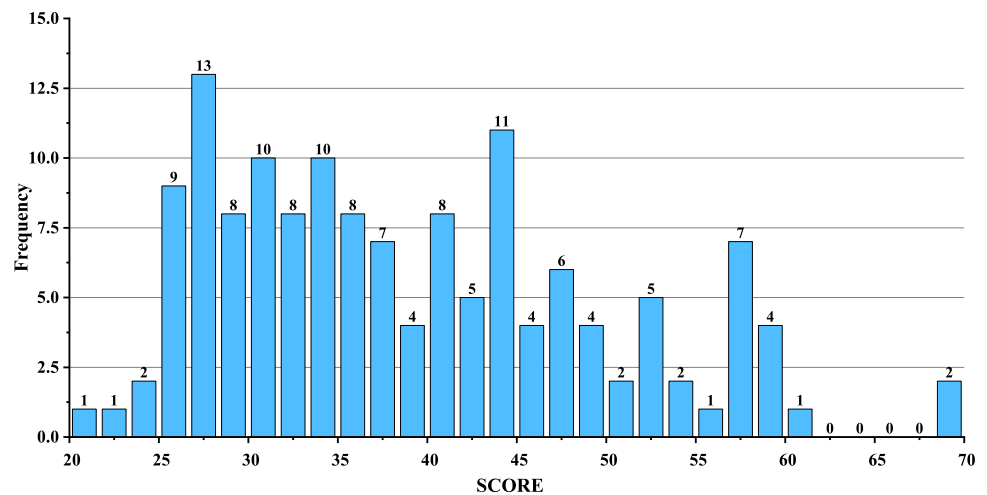


Fig. 11 Water richness zoning map

west and east of the mining area. The northern, central, and a small portion of the eastern parts of the mining area have a lower water richness grade, classified as relatively weak or weak, and thus pose less risk. The areas with strong water richness were the weathered and oxidized zones formed by the coal seam outcrops in the geological report and delineated the scope of the erosion hazard zone.

Method Comparison

In this paper, two weighting methods, the entropy weight method and the improved CRITIC method, were combined, based on Game Theory. To analyze and illustrate the differences between the water richness evaluation models constructed using the weighting method based on Game Theory-based combination weighting and the models constructed using the entropy weight method and the improved CRITIC method alone, we established the entropy weight method-TOPSIS water richness evaluation model and the improved CRITIC method-TOPSIS water richness evaluation model separately, based on the previously extracted data and calculated weights. These models were then used to evaluate the water-richness of the portions of the mining area in the study region. Except for the weighting methods, no other components of the models were altered. The results are presented in Fig. 12.

Comparing the water-richness evaluation maps obtained from the combinatorial weighting method with Fig. 11, we found that the water richness zoning map obtained using the improved CRITIC method showed moderate water richness in the northeastern part of the mining area, while the combined weighting water richness zoning map indicated weak water richness in the same area. On the other hand, the water richness zoning map based on the entropy weight method indicated strong water richness in the central part of the mining area, whereas the combined weighting water richness zoning map showed relatively weak water richness in that area.

Pumping test boreholes L12-2, 06-6, and L10-6 located in the southern, central, and northeastern research areas, respectively, were used to assess the accuracy of the three different methods. The locations of the boreholes and the

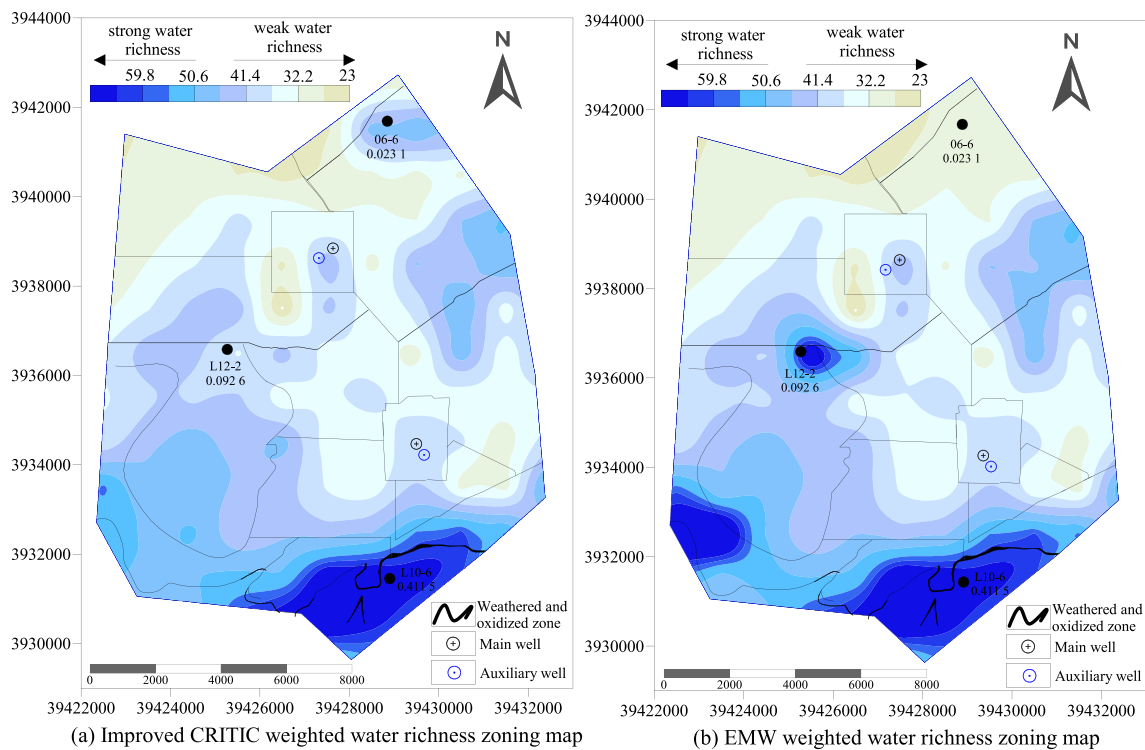


Fig. 12 Water richness zoning map based on single weighting method

specific discharge rates are shown in Fig. 12. The comparison revealed that the evaluation results based on the Game Theory combined weighting-TOPSIS model closely matched the actual data. The main reasons for this are:

- (1) In the water richness evaluation model using the improved CRITIC method for weight assignment, there exists a stability issue with the weight distribution. Specifically, the weight distribution can undergo important changes under the influence of small data fluctuations. After combining and analyzing the contour maps of various indicators, we found that in the northeastern part of the mining area, the data for each indicator was generally stable but with minor fluctuations. Therefore, the improved CRITIC method may have encountered stability issues in weight allocation.
- (2) In the water richness evaluation model using the entropy weight method for weight assignment, the entropy weight method treats different indicators as separate entities without considering the correlation between them, and is overly sensitive to changes in the indicators. Through the analysis of various indicators and their contour maps in the water richness evaluation model, we found differences in the water richness evaluation results and variations in the water richness indicator data in the central part of the mining area. Moreover, the indicators were not completely inde-

pendent of each other, which may have led to a certain degree of error.

- (3) Combining the two weighting methods using Game Theory provides greater comprehensiveness and flexibility. This approach effectively addresses issues such as the interaction and integration among various indicators, as well as fluctuations in indicator data.

Conclusions

- (1) When evaluating the water-richness of the strata overlying coal seams, the main focus is on the water-bearing capacity of the aquifer, its connectivity with the coal seams, and the water-barrier capacity of the strata. The structure of the study area is relatively complex. Based on a comprehensive analysis of the geology, stratigraphy, structure, and lithology of the minefield, four influencing factors were selected to compose the water-conducting channel indexes in terms of structural water control, namely the height of the water-conducting fractured zone, the fault strength index, the fault fractal dimension value, and the fault density. For sedimentary water control, a water barrier capacity index was constructed, including the thickness of the clay layers and the number of sandy-clay interlayers. Also, a water inrush intensity index was established, includ-

- ing the hydraulic pressure of the primary aquifer, the lithological coefficient of sandstones, the equivalent thickness of sandstones, and the interval between the Neogene System and coal seam. These indexes collectively establish an evaluation system for water richness.
- (2) Based on the lithology and structural features of the strata overlying the coal seams in the study area, a water-richness evaluation model was established using Game Theory-based combined weighting and the TOPSIS method. The water richness of the overlying strata of the coal seams in the study area was predicted, and the water richness was presented in a more intuitive manner through scoring. The scoring was divided into five qualitative grades. This allowed for the classification and zoning of water richness in the study area. The results of the water richness evaluation indicate that the overall water richness of the study area is not strong, with most areas exhibiting relatively weak water-richness, mainly in the central and northern parts of the study area. In contrast, the southern and southwestern parts of the study area have greater water richness, validating the previously mentioned weathered and eroded coal seam outcrop areas and delineating the extent of the erosion hazard zone. Additionally, there are small areas of moderate water richness in the northeastern part of the study area. These findings are consistent with actual drilling tests, further validating the accuracy and reliability of the evaluation model. This new evaluation method provides a novel perspective for assessing the water richness of the strata of overlying coal seams, enhancing the scientific rigor and precision of the assessment, and offering robust support for hydrogeological research and safe coal mining.
 - (3) After comparing and analyzing different methods, the water-richness evaluation model established based on Game Theory-based combined weighting and the TOPSIS method effectively addresses the issues of interdependence and integration among data. This model not only comprehensively considers the complex relationships among various influential factors but also enhances the accuracy and reliability of the evaluation results through scientific weight allocation and ranking methods. Ultimately, the evaluation outcomes generated by this approach are more rigorous and precise than other methods, providing a more robust theoretical foundation and practical guidance for the study of water richness in the strata overlying coal seams.
 - (4) Despite the strengths of this study, an important limitation should be acknowledged: slowdowns in processing times when handling extremely large datasets. This can affect the overall efficiency and scalability of the evaluation process. In future research, the model will be optimized to enhance its processing speed for large-

scale data handling. Such improvements will increase its efficiency and general applicability.

Supplementary Information The online version contains supplementary material available at <https://doi.org/10.1007/s10230-024-01018-9>.

Acknowledgements This study was funded by Shandong Provincial Natural Science Foundation (ZR2021MD057).

Data availability All data included in this study are available upon request by contact with the corresponding author.

References

- Arcanjo GS, Costa FC, Ricci BC, Mounteer AH, Melo NML, Cavalcante BF, Araújo AV, Faria CV, Amaral MCS (2020) Draw solution solute selection for a hybrid forward osmosis-membrane distillation module: effects on trace organic compound rejection, water flux and polarization. *Chem Eng J* 400:125857. <https://doi.org/10.1016/j.cej.2020.125857>
- Chen Y, Fan GW, Yin C, Zhang DS, Han XS (2023) Evaluation of roof water richness of water-drenching roadway based on improved AHP-entropy weight coupling. *Coal Eng* 55(12):141–146. <https://doi.org/10.11799/ce202312024>. (in Chinese)
- Diakoulaki K, Mavrotas G, Papayannakis L (1995) Determining objective weights in multiple criteria problems: the critic method. *Comput Oper Res* 22(7):763–770. [https://doi.org/10.1016/0305-0548\(94\)00059-H](https://doi.org/10.1016/0305-0548(94)00059-H)
- Gong HJ, Liu SQ, Zeng YF (2018) Evaluation research on water-richness of aquifer based on BP artificial neural network. *Coal Technol* 37(09):181–182. <https://doi.org/10.13301/j.cnki.ct.2018.09.067>. (in Chinese)
- Huang H (2016) Prediction method of mine inflow and its development. *Coal Sci Technol* 44(S1):127–130.
- Huang L, Gao RZ, Li XA, Gou QS, Hu C (2018) Aquifer water-richness evaluation method based on AHP method and SNMR information fusion. *J Chin Hydrol* 38(1):35–40 (in Chinese)
- Jiang J (2020) Application of DC electric sounding in Quaternary loose aquifer fine exploration of a Shanxi coalmine. *Coal Geol Chin* 32(9):74–78 (in Chinese)
- Jiang AM, Yang H, Zhang M (2012) Study on deterministic mathematical model for predicting water gushing yield of tunnel. *Geotech Investig Surv* 40(06):37–41 (in Chinese)
- Lv AT, Gao YB, Han W, Dong Y, Zhong ZF, Meng QC (2024) Comprehensive credit evaluation of transportation enterprises based on game theory combinatorial weighting -TOPSIS method. *J Shandong U Nat Sc*. <https://doi.org/10.6040/j.issn.1671-9352.0.2023.153>. (in Chinese)
- Shannon CE (1948) A mathematical theory of communication. *Syst Tech J* 27:379–423. <https://doi.org/10.1002/j.1538-7305.1948.tb01338.x>
- Shi LQ, Wang YR, Qiu M, Gao WF (2020) Application of time series model in water inflow prediction of working face. *Coal Geol Explor* 48(3):108–115. <https://doi.org/10.3969/j.issn.1001-1986.2020.03.016>. (in Chinese)
- Shi LQ, Zhao W, Liu TH, Zhai PH, Wang Z, Lv CX (2022) Quantitative evaluation for structure complexity of coal mine field. *Coal Eng* 54(08):142–148. <https://doi.org/10.11799/ce202208025>. (in Chinese)
- Tian LB, Liu F, Chen ZL (2010) The progress and current status of green mining technologies for China's coal resources. *Energy Technol Management* 10(04):140–142

- Tian W, Zou GG, Tang XM, Zeng H (2017) Method of predicting the water abundance of limestone based on AVO technique and pseudo Poisson's ratio attribute. *J China Coal Soc* 42(10):2706–2717. <https://doi.org/10.13225/j.cnki.jccs.2017.0131>. (in Chinese)
- Wang HZ, Hu XW, Shu YF (2010) On the technique of detecting water yield property in seam roof and its application. *Shaanxi Coal* 29(02):70–72 (in Chinese)
- Wang Y, Han J, Gao WF (2017) Water-richness evaluation of Ordovician limestone based on principal component analysis. *Chin Sci* 12(9):1011–1014 (in Chinese)
- Wang J, Hu GL, Zhang L (2022) Evaluation and prediction of temporal and spatial changes of water resources carrying capacity in the Beijing-Tianjin-Hebei region. *China Rural Water Hydropower* 3:69–74. <https://doi.org/10.3969/j.issn.1007-2284.2022.03.011>. (in Chinese)
- Wei JC, Zhao ZC, She DL, Yu GYS, Wu X (2020) Water-abundance evaluation of sandstone aquifer based on lithologic and structural characteristics. *J Shandong U Nat Sci* 39(03):13–23. <https://doi.org/10.16452/j.cnki.sdkjzk.2020.03.002>. (in Chinese)
- Wu Q (2014) Progress, problems and prospects of prevention and control technology of mine water and reutilization in China. *J Chin Coal Soc* 39(5):795–805 (in Chinese)
- Wu Q, Wang Y, Zhao KD, Shen JJ (2017) Water abundance assessment method and application of loose aquifer based on sedimentary characteristics. *J Chin U Min Tech* 46(03):460–466. <https://doi.org/10.13247/j.cnki.jcmt.000679>. (in Chinese)
- Xie Y, Wang J, Jiang XS, Li MH, Xie ZW, Luo JN, Hou GC, Liu F, Wang YH, Zhang MS, Zhu Y, Wang QD, Sun YM, Cao JK (2005) Sedimentary characteristics of cretaceous desert facies in ordos basin and their hydrogeological significance. *Acta Sedimentol Sinica* 23(01):73–83. <https://doi.org/10.3969/j.issn.1000-0550.2005.01.010>. (in Chinese)
- Yang L, Lei FC, Hou EK, Lu B, Feng D, Zhao KX (2023) Zoned prediction of water inflow after dewatering of working face based on water richness zoning of aquifer. *Coal Geol Explor* 51(10):114–123. <https://doi.org/10.12363/issn.1001-1986.23.01.0046>. (in Chinese)
- Yazdani H, Baneshi H, Yaghoubi M (2023) Techno-economic and environmental design of hybrid energy systems using multi-objective optimization and multi-criteria decision making methods. *Energy Convers Manage* 282:116873. <https://doi.org/10.1016/j.enconman.2023.116873>
- Zhang L, He JR (2024) Evaluation of green city development level based on entropy weight-TOPSIS method: taking Jinan City as an example. *J Eng Manag* 38(01):71–76. <https://doi.org/10.13991/j.cnki.jem.2024.01.013>. (in Chinese)
- Zhang LJ, Zhang X (2015) Weighted clustering method based on improved CRITIC method. *Stat Decis* 22:65–68 (in Chinese). <https://doi.org/10.13546/j.cnki.tjyjc.2015.22.018>
- Zhang M, Liu QM, Zhang YT (2018) Water abundance evaluation of coal roof sandstone based on improved Gray extension correlation method. *Min Safe Environ Prot* 45(5):64–68 (in Chinese)
- Zhang X, Liang PY, Chen RR (2020) Evaluation of service innovation ability of regional science and technology service industry: based on the improved CRITIC-VIKOR method. *Sci Technol Manag Res* 40(16):60–69. <https://doi.org/10.3969/j.issn.1000-7695.2020.16.009>. (in Chinese)
- Zhao H, Zhao LL, Tian H, Ding LC, Wang F, Wang ZR, Han CH, Gong WQ, Hou XD (2023) Comprehensive evaluation of water resources carrying capacity in Ankang city based on game theory combination weighting-TOPSIS model. *Geol Resour* 32(05):642–654. <https://doi.org/10.13686/j.cnki.dzyzy.2023.05.015>. (in Chinese)
- Zhu XA, Wei GD (2015) Discussion on the excellent standards of dimensionless methods in entropy method. *Stat Decis* 22(02):12–15. <https://doi.org/10.13546/j.cnki.tjyjc.2015.02.003>. (in Chinese)
- Zuo QT, Zhao ZZ, Wu BB (2020) Evaluation of water resources carrying capacity of nine provinces in Yellow River Basin based on combined weight TOPSIS model. *Water Resour Prot* 36(02):1–7. <https://doi.org/10.3880/j.issn.1004-6933.2020.02.001>. (in Chinese)

Springer Nature or its licensor (e.g. a society or other partner) holds exclusive rights to this article under a publishing agreement with the author(s) or other rightsholder(s); author self-archiving of the accepted manuscript version of this article is solely governed by the terms of such publishing agreement and applicable law.